

Universal Steps Guiding the Branching of the Nuclear Probability Density over Nonadiabatic Electronic Transitions

Guillermo Albareda,^{1,*} Ali Abedi,^{2,†} Ivano Tavernelli,^{3,‡} and Angel Rubio^{2,4,§}

¹*Departament de Química Física & Institut de Química Teòrica i Computacional, Universitat de Barcelona, 08028 Barcelona, Spain*

²*Nano-Bio Spectroscopy Group and ETSF, Dpto. Física de Materiales, Universidad del Pas Vasco, CFM CSIC-UPV/EHU-MPC & DIPIC, 20018 San Sebastian, Spain.*

³*IBM Research GmbH, Zürich Research Laboratory, 8803 Rüschlikon. Switzerland*

⁴*Max Planck Institute for the Structure and Dynamics of Matter and Center for Free-Electron Laser Science, Luruper Chaussee 149, 22761 Hamburg, Germany.*

In the conditional approach to molecular dynamics the electron-nuclear wavefunction is exactly decomposed into an ensemble of nuclear wavepackets governed by conditional time-dependent potential-energy surfaces (C-TDPESs) [G. Albareda, et al., Phys. Rev. Lett. 105, 123002 (2014)]. Employing a one-dimensional model system we show that for strong nonadiabatic couplings the C-TDPESs exhibit steps that bridge between piecewise adiabatic shapes. A detailed analysis of the steps sheds light into the ultimate nature of electron-nuclear correlations and its comparison with the discontinuities that emerge in the exact factorization of the molecular wavefunction brings us to claim their universality in theories without Born-Oppenheimer potential-energy surfaces.

PACS numbers: 31.15.-p,31.15.X-31.50.-x,31.15.A-

The description of correlated electron-nuclear dynamics remains a formidable challenge in condensed-matter physics and theoretical chemistry [1–6]. Relying on the Born-Huang expansion of the full molecular wavefunction, a majority of approaches that provide a numerically accurate description of the so-called “nonadiabatic” processes require the propagation of a set of many-body nuclear wavepackets on a coupled set of Born-Oppenheimer potential-energy surfaces (BOPEs) [7–13]. Whenever electron-nuclear coherence effects are unimportant, efficient mixed quantum-classical propagation techniques can be used [14–20]. However, in order to account for strong correlations, the access to quantum features of the nuclear motion such as spreading, tunnelling or splitting is crucial. Hence, a reliable description of molecular dynamics becomes very expensive due to the calculation of the full BOPEs, a (time-independent) problem that scales exponentially with both the nuclear and electronic degrees of freedom [21–23]. Towards a more efficient description of correlated electron-nuclear dynamics, avoiding the computational costs of calculating the BOPEs and non-adiabatic couplings, two alternative formally exact frameworks, viz. the exact factorization (EF) [24] and the conditional decomposition (CD) [25], have been recently proposed.

The CD approach to molecular dynamics allows for the decomposition of the electron-nuclear wavefunction into an ensemble of nuclear wavefunctions effectively governed by conditional time-dependent potential-energy surfaces (C-TDPESs) [25]. While keeping the theory at the full configuration level, this approach allows for the use of trajectory-based statistical techniques to circumvent the calculation of the BOPEs and nonadiabatic couplings.

Furthermore, this approach avoids artifacts coming from the tracing out of the electronic degrees of freedom and, hence, it allows to draw clear connections between different formally exact frameworks. In this Letter we investigate the generic features of the exact C-TDPESs in the presence of strong nonadiabatic couplings. A major result will be that the exact C-TDPESs exhibit discontinuous steps connecting different BOPEs analogous to paradigmatic features of the effective time-dependent potential that governs the nuclear dynamics in the EF framework. By establishing a formal connection between the CD and the EF frameworks we will discuss the universality of these features in theories without BOPEs.

Throughout this Letter we use atomic units, and electronic and nuclear coordinates are collectively denoted by $\mathbf{r} = \{\mathbf{r}_1, \dots, \mathbf{r}_{N_e}\}$ and $\mathbf{R} = \{\mathbf{R}_1, \dots, \mathbf{R}_{N_n}\}$, where N_e and N_n are the total number of electrons and nuclei. We have recently proved [25] that the full (non-relativistic) electron-nuclear wavefunction $\Psi(\mathbf{r}, \mathbf{R}, t)$ can be exactly decomposed into an ensemble of conditional nuclear wavefunctions, $\psi_\alpha(\mathbf{R}, t) := \int \delta(\mathbf{r}_\alpha(t) - \mathbf{r}) \Psi(\mathbf{r}, \mathbf{R}, t) d\mathbf{r}$, provided that the electronic trajectories $\{\mathbf{r}_\alpha(t) \equiv \mathbf{r}_{1,\alpha}(t), \dots, \mathbf{r}_{N_e,\alpha}(t)\}$ explore the electronic support of $|\Psi(\mathbf{r}, \mathbf{R}, t)|^2$ at any time t [26]. These conditional wavefunctions can be used to reconstruct the full wavefunction (or equivalently any observable) through $\Psi(\mathbf{r}, \mathbf{R}, t) = \hat{D}_\mathbf{r}[\psi_\alpha]$, where $\hat{D}_\mathbf{a}[f(\mathbf{a}_\alpha)] \equiv \sum_{\alpha=1}^{\infty} \delta(\mathbf{a}_\alpha - \mathbf{a}) f(\mathbf{a}_\alpha) / \sum_{\alpha=1}^{\infty} \delta(\mathbf{a}_\alpha - \mathbf{a})$ when $\sum_{\alpha=1}^{\infty} \delta(\mathbf{a}_\alpha - \mathbf{a}) \neq 0$ and it is zero otherwise. Throughout this work we will use quantum trajectories defined through $\mathbf{r}_{\xi,\alpha}(t) = \mathbf{r}_{\xi,\alpha}(t_0) + \int_{t_0}^t \dot{\mathbf{r}}_{\xi,\alpha}(t') dt'$ and $\mathbf{R}_{\nu,\alpha}(t) = \mathbf{R}_{\nu,\alpha}(t_0) + \int_{t_0}^t \dot{\mathbf{R}}_{\nu,\alpha}(t') dt'$, where electronic

and nuclear velocities are given by $\dot{\mathbf{r}}_{\xi,\alpha} = \nabla_{\xi} S|_{\mathbf{r}_{\alpha}, \mathbf{R}_{\alpha}}$ and $\dot{\mathbf{R}}_{\nu,\alpha} = (\nabla_{\nu} S)/M_{\nu}|_{\mathbf{r}_{\alpha}, \mathbf{R}_{\alpha}}$, and S is the phase of the full electron-nuclear wavefunction $\Psi = |\Psi|e^{iS}$ [27, 28]. For the sake of simplicity, we will omit from now on the explicit dependence of the trajectories on time, i.e. $\{\mathbf{r}_{\alpha}\} \equiv \{\mathbf{r}_{\alpha}(t)\}$. In the absence of time-dependent external fields, the molecular system is described by the Hamiltonian $\hat{H} = \hat{T}_e(\mathbf{r}) + \hat{T}_n(\mathbf{R}) + W(\mathbf{r}, \mathbf{R}, t)$, where $\hat{T}_e = -\sum_{\xi=1}^{N_e} \nabla_{\xi}^2/2$ and $\hat{T}_n = -\sum_{\nu=1}^{N_n} \nabla_{\nu}^2/2M_{\nu}$ are the electronic and nuclear kinetic energy operators, and $W(\mathbf{r}, \mathbf{R}, t) = W_{ee}(\mathbf{r}) + W_{nn}(\mathbf{R}) + W_{en}(\mathbf{r}, \mathbf{R})$ denotes the internal Coulombic interactions. The wavefunctions $\psi_{\alpha}(\mathbf{R}, t)$ obey the following equations of motion [25]:

$$id_t \psi_{\alpha}(\mathbf{R}, t) = \left\{ \hat{T}_n(\mathbf{R}) + V_{\alpha}(\mathbf{R}, t) \right\} \psi_{\alpha}(\mathbf{R}, t), \quad (1)$$

where the effective potentials $V_{\alpha}(\mathbf{R}, t) = W_{\alpha}(\mathbf{R}, t) + K_{\alpha}(\mathbf{R}, t) + A_{\alpha}(\mathbf{R}, t)$ are named conditional time-dependent potential energy surfaces (C-TDPESs). Each C-TDPES consists of three terms: the conditional Coulombic potential $W_{\alpha}(\mathbf{R}, t) = W(\mathbf{r}_{\alpha}, \mathbf{R}, t)$, the kinetic correlation potential, $K_{\alpha}(\mathbf{R}, t) = \frac{\hat{T}_e \Psi}{\Psi}|_{\mathbf{r}_{\alpha}}$, and an advective potential, $A_{\alpha}(\mathbf{R}, t) = i \sum_{\xi=1}^{N_e} \frac{\nabla_{\xi} \Psi}{\Psi}|_{\mathbf{r}_{\alpha}} \cdot \dot{\mathbf{r}}_{\xi,\alpha}$. As shown in Eq. (1), each nuclear wavefunction $\psi_{\alpha}(\mathbf{R}, t)$ represents a $3N_n$ -dimensional *slice* of the full molecular wavefunction (taken along the nuclear coordinates) whose evolution is, in general, non-unitary due to the complex nature of the kinetic and advective potentials.

Note that the propagation of the nuclear equations of motion in Eq. (1) does not require the calculation of the BOPESSs. This makes the method particularly advantageous when studying processes that involve many BOPESSs, as in laser-induced dynamics or scattering from metallic surfaces. Since the initial conditions of a trajectory-based simulation can be generated with importance-sampling techniques, conditional decompositions can be exploited to circumvent the problem of storing and propagating a many-particle wave function whose size scales exponentially with the number of particles. In this respect, let us emphasize that the conditional decomposition of the molecular wave function in Eq. (1) is only one case among many other possible conditional decompositions [25, 29–32].

To analyze the C-TDPESs, we decompose V_{α} into real and imaginary parts $V_{\alpha}^{\Re} = W_{\alpha}(R, t) + K_{\alpha}^{\Re} + A_{\alpha}^{\Re}$ and $V_{\alpha}^{\Im} = K_{\alpha}^{\Im} + A_{\alpha}^{\Im}$, where

$$K_{\alpha}^{\Re} = \sum_{\xi=1}^{N_e} Q_{\xi,\alpha}^e + \frac{(\nabla_{\xi} S)^2}{2}|_{\mathbf{r}_{\alpha}}; \quad K_{\alpha}^{\Im} = - \sum_{\xi=1}^{N_e} \frac{\nabla_{\xi} \mathbf{j}_{\xi}}{2|\Psi|^2}|_{\mathbf{r}_{\alpha}}, \quad (2)$$

and

$$A_{\alpha}^{\Re} = - \sum_{\xi=1}^{N_e} \nabla_{\xi} S|_{\mathbf{r}_{\alpha}} \cdot \dot{\mathbf{r}}_{\xi,\alpha}; \quad A_{\alpha}^{\Im} = \sum_{\xi=1}^{N_e} \frac{\nabla_{\xi} |\Psi|^2}{2|\Psi|^2}|_{\mathbf{r}_{\alpha}} \cdot \dot{\mathbf{r}}_{\xi,\alpha}, \quad (3)$$

are respectively the real and imaginary parts of the kinetic and advective correlation potentials. In Eq. (2)

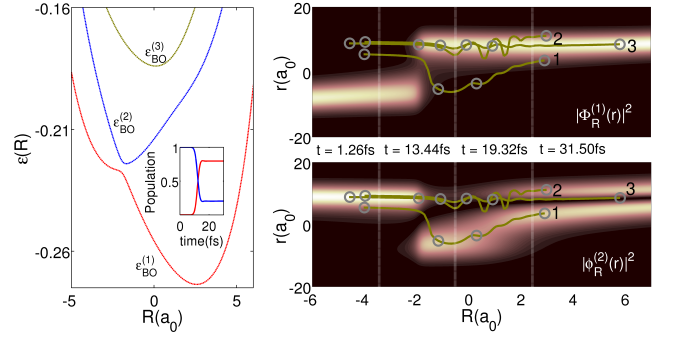


FIG. 1. Left Panel: lowest three BOPESSs $\epsilon_{BO}^{(1)}$ in red, $\epsilon_{BO}^{(2)}$ in blue, and $\epsilon_{BO}^{(3)}$ in green. In the inset: adiabatic populations as a function of time. Right Panel: Squared value of the Born-Oppenheimer states $\Phi_R^{(1)}(r)$ and $\Phi_R^{(2)}(r)$ along with the evolution of three selected trajectories $\{r_{\alpha}(t), R_{\alpha}(t)\}$ labeled $\alpha = 1, 2, 3$. The position of these trajectories at four different times is also show (in gray circles) for later reference.

we have respectively defined the ξ -th components of the so-called electronic quantum potential [27, 28] and the current probability density as $Q_{\xi,\alpha}^e = -\frac{1}{2} \frac{\nabla_{\xi}^2 |\Psi|}{|\Psi|}|_{\mathbf{r}_{\alpha}}$ and $\mathbf{j}_{\xi} = |\Psi|^2 \nabla_{\xi} S$. While the classical kinetic potential, $(\nabla_{\xi} S)^2/2|_{\mathbf{r}_{\alpha}}$, is in general a smooth function of the nuclear coordinates, we expect the quantum contributions, $Q_{\xi,\alpha}^e$ and K_{α}^{\Im} , to be rather “discontinuous” because of their dependence on the inverse of the conditional nuclear probability density. Notice that these last two quantities are implicit functions of the electronic coordinates. Specifically, the electronic quantum potential $Q_{\xi,\alpha}^e$ accounts for changes of the curvature of the full probability density along the electronic coordinates (as a function of the nuclear positions). Alternatively, K_{α}^{\Im} describes the dispersion (e.g. spreading or splitting) of the full wavefunction in the electronic direction. Both contributions become large in the vicinity of a node, and thus, they will be important whenever the full probability density splits apart along the electronic coordinates. The advective correlations in Eq. (3) are weighted by electronic velocities, $\dot{\mathbf{r}}_{\xi,\alpha}$, and hence, they will be significant only during a fast reconfiguration of the electronic degrees of freedom.

To study the features of the exact C-TDPESs during nonadiabatic processes in the CD approach, we employ the model introduced by Shin and Metiu [33], which consists of three ions and a single electron. Two ions are fixed at a distance $L = 19.0a_0$, and the third ion and the electron are free to move in one dimension along the line joining the fixed ions. The Hamiltonian for this system reads:

$$\hat{H}(r, R) = -\frac{1}{2} \frac{\partial^2}{\partial r^2} - \frac{1}{2M} \frac{\partial^2}{\partial R^2} + \frac{1}{|\frac{L}{2} - R|} + \frac{1}{|\frac{L}{2} + R|}$$

$$- \frac{\text{erf}\left(\frac{|R-r|}{R_f}\right)}{|R-r|} - \frac{\text{erf}\left(\frac{|r-\frac{L}{2}|}{R_r}\right)}{|r-\frac{L}{2}|} - \frac{\text{erf}\left(\frac{|r+\frac{L}{2}|}{R_l}\right)}{|r+\frac{L}{2}|}, \quad (4)$$

where the symbols \mathbf{r} and \mathbf{R} are replaced by r and R , and the coordinates of the electron and the movable nucleus are measured from the center of the two fixed ions. We choose the remaining parameters to be the same as in reference [34], i.e. $M = 1836\text{a.u.}$ and $R_f = 5.0a_0$, $R_l = 4.0a_0$, and $R_r = 3.1a_0$ such that the first BOPEs, $\epsilon_{BO}^{(1)}$, is strongly coupled to the second, $\epsilon_{BO}^{(2)}$, around $R_{ac} = -2a_0$. The coupling to the rest of the BOPEs is negligible. Note that the time-independent electronic problem is fully characterized through the so-called electronic Hamiltonian, i.e. $(\hat{T}_e + W)\Phi_R^{(j)}(r) = \epsilon_{BO}^{(j)}(R)\Phi_R^{(j)}(r)$. We suppose the system to be initially excited to $\epsilon_{BO}^{(2)}$ and the initial nuclear wavefunction to be a Gaussian wavepacket with $\sigma = 1/\sqrt{2.85}$, centered at $R = -4.0a_0$, i.e. the initial full wavefunction is $\Psi(r, R, t_0) = A e^{-(R+4)^2/\sigma^2} \Phi_R^{(2)}(r)$ with A being a normalization constant. On the left panel of Fig. 1 we show the first three BOPEs together with the evolution of the adiabatic populations (in the inset). The right panel of Fig. 1 shows the first two Born-Oppenheimer states $\Phi_R^{(1)}(r)$ and $\Phi_R^{(2)}(r)$ along with the evolution of three selected trajectories $\{r_\alpha, R_\alpha\}$ labeled $\alpha = 1, 2, 3$. Analyzed below, in Fig. 2 we present four time snapshots containing relevant information about the \mathbb{C} -TDPEs as well as the conditional nuclear wavefunctions. For the sake of clarity we also define approximated real and imaginary components of \mathbb{C} -TDPEs respectively as $V_\alpha^{\Re} = Q_\alpha^e + W_\alpha$ and $V_\alpha^{\Im} = K_\alpha^{\Im}$.

At the initial time ($t_0 = 0\text{fs}$), due to the choice of $\Psi(r, R, t_0)$, the \mathbb{C} -TDPEs are real, α -independent, and by construction all equal to the first excited BOPE $\epsilon_{BO}^{(2)}$:

$$V_\alpha = \frac{\hat{T}_e \Phi_R^{(2)}(r)}{\Phi_R^{(2)}(r)} \Big|_{r_\alpha} + W_\alpha = V_{\alpha,app}^{\Re} = \epsilon_{BO}^{(2)}, \quad \forall \alpha \quad (5)$$

where we used that $Q_\alpha^e(R, t_0) = \hat{T}_e \Phi_R^{(2)}(r)/\Phi_R^{(2)}(r)$ when $\partial_r S = 0$ (a more detailed analysis of the \mathbb{C} -TDPEs in terms of the Born-Huang expansion of the molecular wavefunction can be found in SM A). Since $\Psi(r, R, t_0)$ is not an eigenstate of the Hamiltonian in (4), it evolves in time. As it is made clear in the right panels of Fig. 1, at $t = 13.44\text{fs}$, the trajectories (r_2, R_2) and (r_3, R_3) , associated respectively with the conditional wavefunctions ψ_2 and ψ_3 , are running straight (i.e. $\dot{r}_{2,3} \approx 0$) from the support of $\Phi_R^{(2)}(r)$ to fall in the support of $\Phi_R^{(1)}(r)$. For $\alpha = 2, 3$ the \mathbb{C} -TDPEs are real ($V_{2,3}^{\Im} = 0$) and satisfy $V_{2,3} \approx V_{2,3,app}^{\Re}$, with $Q_{2,3}^e(R < R_{ac}) \approx \hat{T}_e \Phi_R^{(2)}(r)/\Phi_R^{(2)}(r)$ and $Q_{2,3}^e(R > R_{ac}) \approx \hat{T}_e \Phi_R^{(1)}(r)/\Phi_R^{(1)}(r)$. Therefore, as can be seen from Fig. 2 (bottom left panel), the \mathbb{C} -TDPEs resemble diabatic potential-energy surfaces, coinciding with $\epsilon_{BO}^{(2)}$ for $R < R_{ac}$ and smoothly going

through the avoided crossing region to follow $\epsilon_{BO}^{(1)}$ for $R > R_{ac}$. Conversely, trajectory (r_1, R_1) tunnels from one Coulomb potential well W_α to the other, staying most of the time in the support of $\Phi_R^{(2)}(r)$. The velocity \dot{r}_1 is now large due to the fast reconfiguration of the electronic degrees of freedom, and hence V_1 shows important advective contributions. Notice also that both V_1^{\Re} and V_1^{\Im} show steep peaks that originate in the full configuration space as the full probability density starts to split up along the electronic coordinates (left panels b) and c) of Fig. 2). At the later time $t = 19.32\text{fs}$, the advective correlation and classical kinetic terms become once more negligible, and therefore $V_\alpha \approx V_{\alpha,app}^{\Re} + V_{\alpha,app}^{\Im}$. While (r_1, R_1) stays preferentially in the support of $\Phi_R^{(2)}(r)$, the trajectories (r_2, R_2) and (r_3, R_3) are mainly sampling the support of $\Phi_R^{(1)}(r)$ (see the right panel of Fig. 1). The conditional wavefunctions ψ_1 , ψ_2 and ψ_3 are now linear combinations of $\Phi_R^{(2)}(r)$ or $\Phi_R^{(1)}(r)$ (possibly showing contributions from higher energetic Born-Oppenheimer states) [35]. This mixture leads to the formation of the step observed for V_1 around $R = 1.5a_0$, and also to wiggles accompanying in the \mathbb{C} -TDPEs V_2 and V_3 . All these features indicate the nonadiabatic nature of the conditional wavefunctions and can be directly associated with the formation of nodes in the full probability density. Concretely, as shown in panels b) and c) of Fig. 2, the splitting of the full probability density can be understood as the result of the formation of dynamical nodes (originating from kinetic correlations) that move across the full configuration space as if they were knife edges. Finally, at time $t = 31.5\text{fs}$, the full molecular wavefunction has been split both along the electronic and nuclear directions. While the three conditional wavefunctions, ψ_1 , ψ_2 and ψ_3 , still embody contributions from both $\Phi_R^{(1)}(r)$ and $\Phi_R^{(2)}(r)$, these contributions are now very well separated along the nuclear coordinates with a minimum at around $R_{sp} = 4a_0$ (see also Fig. 1, right panel). For nuclear coordinates less than R_{sp} , the support of the full probability density perfectly fits in the support of the first excited Born-Oppenheimer state $\Phi_R^{(2)}(r)$, while for $R > R_{sp}$ it mainly falls in the ground state $\Phi_R^{(1)}(r)$. As a direct consequence, the quantum electronic potential acquires a discontinuity, i.e. $Q_\alpha^e(R < R_{sp}) \approx \hat{T}_e \Phi_R^{(2)}(r)/\Phi_R^{(2)}(r)$ while $Q_\alpha^e(R > R_{sp}) \approx \hat{T}_e \Phi_R^{(1)}(r)/\Phi_R^{(1)}(r)$. The real parts of the \mathbb{C} -TDPEs are therefore piecewise connecting adiabatic surfaces, i.e. $V_\alpha^{\Re} \approx V_{\alpha,app}^{\Re} \approx \epsilon_{BO}^{(1)}$ for $R > R_{sp}$, and $V_\alpha^{\Re} \approx V_{\alpha,app}^{\Re} \approx \epsilon_{BO}^{(2)}$ for $R < R_{sp}$ (the reader is again referred to SM A for further discussion). In the transition between this two regions (at around R_{sp}), the conditional wave functions ψ_1 , ψ_2 and ψ_3 become linear combinations of (at least) the lowest two adiabatic electronic states. As a result, the \mathbb{C} -TDPEs exhibit abrupt peaks, both real and imaginary, mainly originating from the potentials Q_α^e and K_α^{\Im} . In the full configuration space (left panels in

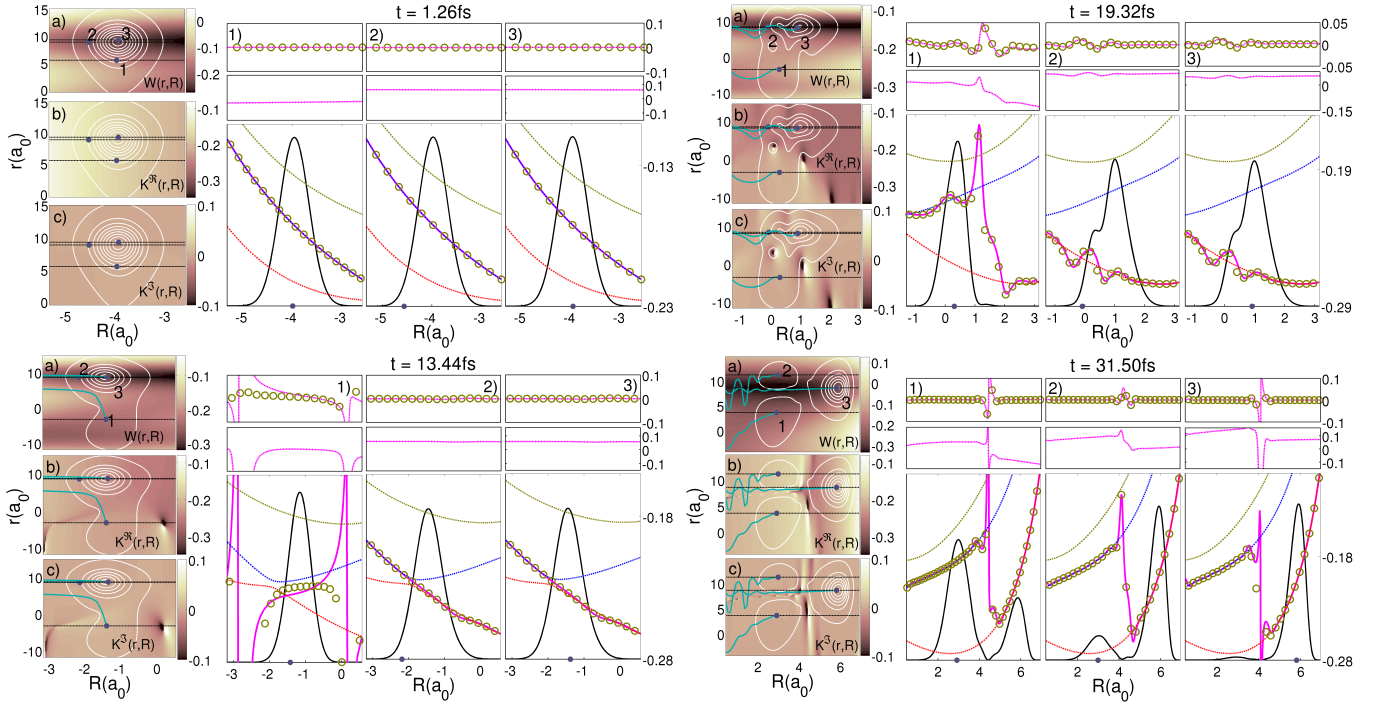


FIG. 2. LEFT PANELS: Contour lines of the full electron-nuclear probability density (in white) together with three conditional wavefunctions, $\psi_1(R, t)$, $\psi_2(R, t)$, and $\psi_3(R, t)$ (dotted black lines), defined along with the trajectories $\{r_{\alpha=1,2,3}, R_{\alpha=1,2,3}\}$ (in cyan). In the background (in copper color scale), full configuration dependence of a) the electron-nuclear potential energy $W(r, R)$, and b) and c) respectively the real and imaginary components of the kinetic correlation potential $K^{\mathfrak{R}}(r, R, t)$. RIGHT PANELS: In 1), 2) and 3) (bottom) we display the conditional probability densities $|\psi_{\alpha=1,2,3}(R, t)|^2$ (black solid-lines) along with the first three BOPEs (dotted red = $\epsilon_{BO}^{(1)}$, blue = $\epsilon_{BO}^{(2)}$, and green = $\epsilon_{BO}^{(3)}$ lines) and the real part of the C-TDPESs $V_{\alpha}^{\mathfrak{R}} = W_{\alpha} + K_{\alpha}^{\mathfrak{R}} + A_{\alpha}^{\mathfrak{R}}$ (in magenta). For comparison we also show the potential $V_{\alpha, app}^{\mathfrak{R}} = Q_{\alpha}^e + W_{\alpha}$ (green circles). In 1), 2) and 3) (middle): Electronic quantum potential alone Q_{α}^e . In 1), 2) and 3) (top): Imaginary part of the C-TDPESs $V_{\alpha}^{\mathfrak{I}} = K_{\alpha}^{\mathfrak{I}} + A_{\alpha}^{\mathfrak{I}}$ (magenta line) along with the approximated potential $V_{\alpha, app}^{\mathfrak{I}} = K_{\alpha}^{\mathfrak{I}}$ alone (green circles).

Fig. 2), these features are now directly translated into deep wells/barriers that keep the full probability density well separated into three pieces.

Recently, the concept of the TD PES has been used to shed light into the origins of the branching of the nuclear probability density in nonadiabatic transitions. In [34], Abedi et al. report properties of the TD PES that closely match the merits that we have just described for the ensemble of C-TDPESs: far from the region of avoided crossings (when the nonadiabatic couplings are negligible) the TD PES coincide with the adiabatic BOPEs, while in their neighborhood exhibits nearly discontinuous steps that connect two different adiabatic BOPEs. The same behavior was also observed for the C-TDPESs derived in this work and therefore it is worth investigating if these discontinuities have a common, universal origin. To this end, by virtue of the EF theorem, we rewrite the conditional nuclear wavefunction as a direct product of conditional electronic and nuclear wavefunctions, i.e., $\psi_{\alpha}(\mathbf{R}, t) = \Phi_{\mathbf{R}}(\mathbf{r}_{\alpha}, t)\chi(\mathbf{R}, t)$. By inserting this Ansatz into Eq. (1), equations of motion for both electronic and nuclear factors can be derived. Here, the nuclear wavefunction, $\chi(\mathbf{R}, t)$, plays a

central role in establishing a relation between the EF and CD frameworks. For the model system studied here [36], the equation of motion for $\chi(\mathbf{R}, t)$ simply reads $i\partial_t\chi(\mathbf{R}, t) = \{\hat{T}_n(\mathbf{R}) + \epsilon(\mathbf{R}, t)\}\chi(\mathbf{R}, t)$, where the exact TD PES, $\epsilon(\mathbf{R}, t)$, effectively governs the nuclear dynamics and can be written in terms of the C-TDPESs as:

$$\epsilon(\mathbf{R}, t) = \frac{\int \hat{\mathcal{D}}_{\mathbf{r}}[|\psi_{\alpha}|^2 V_{\alpha}] d\mathbf{r}}{\int \hat{\mathcal{D}}_{\mathbf{r}}[|\psi_{\alpha}|^2] d\mathbf{r}} + O(M_n^{-1}) + \epsilon_{\text{gd}}(\mathbf{R}, t). \quad (6)$$

The third term on the r.h.s of Eq. (6), $\epsilon_{\text{gd}}(\mathbf{R}, t)$, depends on the specific choice of the gauge, while the second term, $O(M_n^{-1})$, it is most of the time negligible because it depends on the inverse of the nuclear mass (see SM B). We are left with the first term on the r.h.s of Eq. (6), which establishes a direct connection between the TD PES concept, i.e., a single function of the nuclear coordinates and time, and the C-TDPESs, which are, one-by-one, functions of the nuclear coordinates and time that depend parametrically on the electronic degrees of freedom through the trajectories $\{\mathbf{r}_{\alpha}\}$. As stated in Eq. (6), in the TD PES of the EF approach, discontinuities can be understood to emerge through an ensemble average of C-

TDPEs, V_α , which are integrated along the conditional probability densities $|\psi_\alpha|^2$ and weighted afterwards by the nuclear probability density, $\int \hat{\mathcal{D}}_{\mathbf{r}}[|\psi_\alpha|^2]d\mathbf{r} = \int |\Psi|^2 d\mathbf{r}$.

Hence, the main difference between the BOPEs and the effective time-dependent potentials that arise in the EF and CD frameworks, is that the first are defined independently from the nature and the position of the total electron-nuclear wavefunction, while in the time-dependent case, the effective potentials have a direct dependence on the full wavefunction (either through the first term in the r.h.s of Eq. (6) in the EF framework or through the quantum potential in Eq. (2) in the CD framework), which can induce discontinuities. Within the Born-Oppenheimer picture, the nuclear wavepacket can populate different BOPEs and reproduce in this way coherent wavepacket branching during a nonadiabatic process. In the EF or in the CD discussed here the same physics seems to be universally described by abrupt steps in the effective time-dependent potentials that drive the nuclear wavepacket dynamics. These steps connect different portions of the underlying BOPEs, splitting the support of the nuclear wavepacket into subsets that are associated, piecewise, to different portions of the corresponding BOPEs.

To summarize, we have reported discontinuities in the exact \mathbb{C} -TDPEs for the specific situation where, according to the standard Born-Oppenheimer picture, the nuclear wavepacket splits at the avoided crossing of two BOPEs. The \mathbb{C} -TDPEs are the only potentials that govern the dynamics of the conditional nuclear wavefunctions and, therefore, provide us with an alternative way of visualizing and interpreting nonadiabatic processes without the need of BOPEs or nonadiabatic couplings. Our study reveals that the shape and position of discontinuous steps connecting different BOPEs is mainly dictated by the electronic quantum potential, Q_α^e , which can be understood as a clear-cut signature of the ultimate quantum nature of electron-nuclear correlations. In our analysis we have also identified a very close correspondence between the \mathbb{C} -TDPEs and the effective potentials that arises in the EF approach, both showing the same kind of steps during the branching of the nuclear probability density. A formal connection between the CD and the EF frameworks brought us to discuss on the universality of these discontinuities in molecular dynamics theories without BOPEs. In this respect, it is worth mentioning that other attempts to reduce the complexity of the time-dependent Schrödinger equation, such as in time-dependent density-functional theory, also lead to the emergence of striking discontinuities in the effective time-dependent potentials that govern the reduced variables of interest. This is the case, e.g., in the field of electron-electron correlated dynamics, where the nature of such discontinuities is currently under study [37–39].

ACKNOWLEDGEMENTS

G.A acknowledges financial support from the Beatriu de Pinós program through the Project: 2014 BP-B 00244. A.A acknowledges ... I.T acknowledges the Swiss National Science Foundation (SNF) through Grant No. 200021-146396 and the COST Actions CM1204 (XLIC). A.R acknowledges financial support from the European Research Council Advanced Grant DYNamo (ERC-2010-AdG-267374), Spanish Grant (FIS2013-46159-C3-1-P), Grupos Consolidados UPV/EHU del Gobierno Vasco (IT578-13) and COST Actions CM1204 (XLIC) and MP1306 (EUSpec).

* albarda@ub.edu

† aliabedik@gmail.com

‡ ita@zurich.ibm.com

§ angel.rubio@mpsd.mpg.de

- [1] J. Clark, T. Nelson, S. Tretiak, G. Cirimi, and G. Lanzani, *Nature Physics* **8**, 225 (2012).
- [2] X. Zhou, P. Ranitovic, C. Hogle, J. Eland, H. Kapteyn, and M. Murnane, *Nature Physics* **8**, 232 (2012).
- [3] S. R. Leone, C. W. McCurdy, J. Burgdörfer, L. S. Cederbaum, Z. Chang, N. Dudovich, J. Feist, C. H. Greene, M. Ivanov, R. Kienberger, *et al.*, *Nature Photonics* **8**, 162 (2014).
- [4] F. Lépine, M. Y. Ivanov, and M. J. Vrakking, *Nature Photonics* **8**, 195 (2014).
- [5] R. Boge, C. Cirelli, A. Landsman, S. Heuser, A. Ludwig, J. Maurer, M. Weger, L. Gallmann, and U. Keller, *Physical review letters* **111**, 103003 (2013).
- [6] M. Corrales, J. González-Vázquez, G. Balerdi, I. Solá, R. de Nalda, and L. Bañares, *Nature chemistry* **6**, 785 (2014).
- [7] I. Tavernelli, *Accounts of chemical research* **48**, 792 (2015).
- [8] M. Persico and G. Granucci, *Theoretical Chemistry Accounts* **133**, 1 (2014).
- [9] B. Lasorne, G. A. Worth, and M. A. Robb, in *Molecular Quantum Dynamics* (Springer, 2014) pp. 181–211.
- [10] W. Domcke and D. R. Yarkony, *Annual review of physical chemistry* **63**, 325 (2012).
- [11] J. C. Tully, *The Journal of chemical physics* **137**, 22A301 (2012).
- [12] D. Truhlar, in *The Reaction Path in Chemistry: Current Approaches Understanding Chemical Reactivity*, Vol. 16, edited by D. Heidrich (Springer Netherlands, 1995) pp. 229–255.
- [13] B. F. E. Curchod, U. Rothlisberger, and I. Tavernelli, *ChemPhysChem* **14**, 1314 (2013).
- [14] J. C. Tully, *J. Chem. Phys.* **93**, 1061 (1990).
- [15] J. C. Tully, *Farad. Discuss.* **110**, 407 (1998).
- [16] R. Kapral and G. Ciccotti, *The Journal of chemical physics* **110**, 8919 (1999).
- [17] M. Persico and G. Granucci, *Theoretical Chemistry Accounts* **133**, 1 (2014).
- [18] S. Sawada and H. Metiu, *J. Chem. Phys.* **84**, 227 (1986).

- [19] T. J. Martinez, M. Ben-Nun, and R. D. Levine, *J. Phys. Chem.* **100**, 7884 (1996).
- [20] J. Zheng, X. Xu, R. Meana-Paneda, and D. G. Truhlar, *Chem. Sci.* **5**, 2091 (2014).
- [21] I. Burghardt, H.-D. Meyer, and L. S. Cederbaum, *J. Chem. Phys.* **111**, 2927 (1999).
- [22] M. Beck, A. Jekle, G. Worth, and H.-D. Meyer, *Phys. Rep.* **324**, 1 (2000).
- [23] H.-D. Meyer and G. A. Worth, *Theor. Chem. Acc.* **109**, 251 (2003).
- [24] A. Abedi, N. T. Maitra, and E. K. U. Gross, *Phys. Rev. Lett.* **105**, 123002 (2010).
- [25] G. Albareda, H. Appel, I. Franco, A. Abedi, and A. Rubio, *Phys. Rev. Lett.* **113**, 083003 (2014).
- [26] The electronic support of the full probability density $|\Psi(\mathbf{r}, \mathbf{R}, t)|^2$ can be defined as: $\text{supp}(|\Psi(\mathbf{r}, \mathbf{R}, t)|^2) = \{\mathbf{r} \in \mathbf{r} \mid |\Psi(\mathbf{r}, \mathbf{R}, t)|^2 > \lambda\}$, where λ denotes a given lower bound of the probability density.
- [27] X. Oriols and J. Mompart, *Applied Bohmian Mechanics: From Nanoscale Systems to Cosmology* (Pan Stanford, 2012).
- [28] A. Benseny, G. Albareda, S. Sanz, J. Mompart, and X. Oriols, *The European Physical Journal D* **68**, 286 (2014), 10.1140/epjd/e2014-50222-4.
- [29] G. Albareda, J. M. Bofill, I. Tavernelli, F. Huarte-Larraaga, F. Illas, and A. Rubio, *The Journal of Physical Chemistry Letters* **6**, 1529 (2015), PMID: 26263307, <http://dx.doi.org/10.1021/acs.jpcclett.5b00422>.
- [30] G. Albareda, J. Suñé, and X. Oriols, *Phys. Rev. B* **79**, 075315 (2009).
- [31] G. Albareda, D. Marian, A. Benali, S. Yaro, N. Zangh, and X. Oriols, *J. Comp. Electr.* **12**, 405 (2013).
- [32] X. Oriols, *Phys. Rev. Lett.* **98**, 066803 (2007).
- [33] S. Shin and H. Metiu, *J. Chem. Phys.* **102**, 9285 (1995).
- [34] A. Abedi, F. Agostini, Y. Suzuki, and E. K. U. Gross, *Phys. Rev. Lett.* **110**, 263001 (2013).
- [35] As shown in SM A, the conditional wavefunctions can be always written as a linear combination of Born-Oppenheimer states, i.e. $\psi_\alpha(r, t) = \sum_j C_j(R, t) \Phi_R^{(j)}(r_\alpha)$.
- [36] In the EF approach the coupling between the nuclear and the electronic degrees of freedom is exactly mediated by the TD PES and time-dependent Berry connection up to a gauge transformation. For one-dimensional problems, i.e. if there is only one nuclear degree of freedom, the gauge can be fixed such that the Berry phase is always zero [?].
- [37] P. Elliott, J. I. Fuks, A. Rubio, and N. T. Maitra, *Physical review letters* **109**, 266404 (2012).
- [38] K. Luo, P. Elliott, and N. T. Maitra, *Physical Review A* **88**, 042508 (2013).
- [39] K. Luo, J. I. Fuks, E. D. Sandoval, P. Elliott, and N. T. Maitra, *The Journal of chemical physics* **140**, 18A515 (2014).